Low sedimentary accumulation of lead caused by weak downward export of organic matter in Hudson Bay, northern Canada

Benoit Thibodeau, Christophe Migon, Aurélie Dufour, André Poirier, Xavier Mari, Bassam Ghaleb, Louis Legendre

Low sedimentary accumulation of lead caused by weak downward export of organic matter in Hudson Bay, northern Canada

Benoit Thibodeau[1,2], Christophe Migon[3], Aurélie Dufour[3], André Poirier[4], Xavier Mari[3,5], Bassam Ghaleb[4] and Louis Legendre[3]

[1]Department of Earth Sciences, The University of Hong Kong, Pokfulam Road, Hong Kong

[2]Swire Institute for Marine Science, The University of Hong Kong, Cape d'Aguilar Road, Shek O, Hong Kong SAR

[3]Sorbonne Universités, UPMC, Université Paris 06, CNRS, Laboratoire d'Océanographie de Villefranche-sur-mer (LOV), 181 Chemin du Lazaret, 06230 Villefranche-sur-Mer, France

[4]Geotop, Université du Québec à Montréal, Montréal, Canada

[5]Aix Marseille Université, CNRS/INSU, Université de Toulon, IRD, Mediterranean Institute of Oceanography (MIO) UM 110, 13288, Marseille, France

Keywords: Vertical transfer, particulate matter, oligotrophy, ocean, climate change; carbon budget

Abstract

Atmospheric input of anthropogenic lead increased globally over the last centuries. The present study shows that the concentrations of lead in sediment cores from low-productivity Hudson Bay, northern Canada, remained relatively constant over the last centuries. The lack of imprint of the increased anthropogenic lead input in this marine environment is not consistent with the increased lead concentrations in nearby lakes over the same period. In addition, the observed trend in lead isotopic composition in our cores suggests an apparent progressive overprint of anthropogenic lead during the 1900's. In other words, isotopes clearly registered the increasingly anthropogenic nature of lead in the sedimentary record, but total lead concentrations remained constant, indicating that some process limited the export of lead to the sediment. These observations point to a long-term limitation of the downward export of particles in Hudson Bay. Given that the source of lead was the same for both Hudson Bay and neighboring high-productivity lakes, we hypothesize that the very low primary productivity of Hudson Bay waters was responsible for the low vertical export of lead to marine sediments. We further propose that primary productivity is the most important factor that generally drives the vertical export of particulate matter, and thus hydrophobic contaminants, in near-oligotrophic marine environments.

1. Introduction

Atmospheric transportation of anthropogenic contaminants over thousands of kilometers was reported in the late 1970s as the main mechanism explaining the presence of contaminants at high latitude (Rahn et al. 1977; Barrie et al. 1981). However, the precise mechanisms by which insoluble contaminants deposited at the water surface are exported to depth are still not completely resolved. The settling velocity of individual atmospheric particles with a diameter <5 μm (e.g. dust, sea spray, volcanic ash, anthropogenic material (De Angelis and Gaudichet 1991)) is null or very low in seawater, based on Stokes's law (Buat-Ménard et al. 1989), and their removal from the surface ocean depends on their aggregation with larger particulate biogenic material. The adsorption/aggregation of lithogenic atmospheric material (mostly dust) on/with organic particles are likely to increase the density, and thus the settling velocity of the resulting aggregates (Deuser et al. 1983; Fowler et al. 1987; Alldredge and Silver 1988; Jackson and Burd 1998; Armstrong et al. 2002; Francois et al. 2002; Turner 2002; Burd and Jackson 2009). However, recent studies indicate that, even if this 'ballast effect' probably increases the settling velocity of the sinking material, it may not be the main determinant of the downward export flux (Passow 2004; Heimbürger et al. 2014).

Tight coupling between primary productivity and downward fluxes of particulate organic carbon (POC) has been observed in various marine regions (Gačić et al. 2002; Migon et al. 2002; Boyce et al. 2010; Passow and Carlson 2012; Yool et al. 2013; Turner 2015). This indicates that biological productivity can lead to efficient export of atmospheric material to the sediment by inclusion of biogenic material in mineral-organic aggregates. Given that phytoplankton dynamics is controlled by nutrient availability, the environmental conditions that control limiting nutrients ultimately control the downward export of POC (Lampitt et al. 2010; Heimbürger et al. 2013).

Climate in the Arctic and more generally at high latitudes underwent dramatic changes during the past decades (Macdonald et al. 2005). The 20th century was the warmest period in the Arctic in at least 44,000 years (Miller et al. 2013), and environmental changes included increases in precipitation and river discharge as well as declines in snow cover and sea-ice extent (ACIA 2004). While the effects of such changes on primary productivity could be variable over Arctic shelves (Michel et al. 2015), they may have important consequences on the rates of contaminant scavenging and export from surface to deep water. For example, Outridge et al. (2007) suggested

74 that the 20th century increase in the accumulation of Hg in the sediment of a Canadian high Arctic
75 lake had largely been driven by an increase in autochthonous primary productivity since 1854.
76 In the present study, we hypothesized that low primary productivity was the main forcing
77 factor that determined the sedimentation of atmospherically-deposited matter in Hudson Bay
78 during the last centuries. To test this hypothesis, we investigated the concentration and isotopic
79 signature of Pb in two sediment cores from Hudson Bay, and compared these values with already
80 published sedimentary records from nearby high-productivity lakes (Outridge et al. 2002). We
81 used Pb because its multiple isotopes allow the identification of sources. Moreover, the pollution
82 history of Pb is well documented, especially around Hudson Bay where Pb was measured in lake
83 sediments. Our hypothesis would be rejected if (1) the sedimentary accumulation of Pb during
84 the last century were the same in the sedimentary records of both low-productivity Hudson Bay
85 and high-productivity nearby lakes, thus indicating that primary productivity did not play a key
86 role in the vertical export of Pb, or (2) the recent isotopic composition of records from Hudson
87 Bay and surrounding lakes were not recording the same anthropogenic signal.
88
89 **2. Materials and Methods**
90 *2.1. Study area*
91 Hudson Bay has an area of about 841,000 km^2, an average depth of 125 m (maximum
92 depth of 250 m), and slopes generally less than 2 degrees (Prinsenberg 1986). Dense cold saline
93 water enters the Bay from the northwest (Hudson Strait and Foxe Basin, located in the north of
94 Hudson Bay; Fig. 1). Circulation inside the Bay is cyclonic, with surface currents averaging
95 5 cm s^{-1} in summer, and 2-3 cm s^{-1} in winter when the Bay is ice-covered (Saucier and Dionne
96 1998). There is a surface outflow of relatively warm and fresh water to the northeast of the Bay
97 towards Hudson Strait. Estimates of the residence time of surface (fresh) water are quite variable
98 in the literature, i.e. they range from the order of one month to more than 6 years (Prinsenberg
99 1984; Jones and Anderson 1994; Granskog et al. 2009). Many rivers discharge freshwater in the
100 southern part of Hudson Bay, causing a strong latitudinal surface salinity gradient. The annual
101 discharge (710 km^3 yr^{-1}) is equivalent to an annual freshwater yield of about 65 cm over the
102 whole bay (Prinsenberg 1986). This freshwater inflow has a profound influence on the physical,
103 chemical and biological properties of the Bay because it fosters stratification of the water column,
104 which usually reduces vertical mixing and thus upward transport of nutrients (Prinsenberg 1986).

Although the intense stratification may suggest that Hudson Bay is oligotrophic, a recent study indicates that even if the riverine inputs are relatively minor sources of nitrate, the inputs of freshwater favor rather than impede primary productivity inshore by indirectly fostering the entrainment and upwelling of deeper water to the surface (Kuzyk et al. 2010a). Because Hudson Bay is semi-enclosed within the Canadian Shield, its geochemical characteristics are strongly influenced by local factors such as the geological substrates that are drained by river runoff, wet and dry atmospheric depositions, and seasonal sea-ice formation and melt.

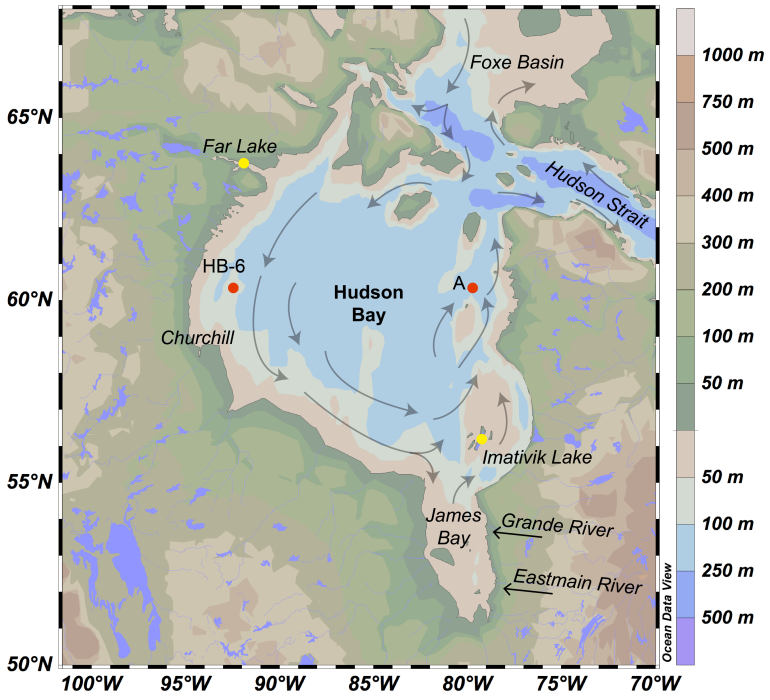

Fig. 1: Map of Hudson Bay with major currents. The two red dots indicate the locations of our two sediment cores at about 60°N (Stations HB-6 and A), the yellow dots indicate the locations of the two lakes to which our data are compared in the discussion and the two straight arrows on the eastern side of James Bay represent major river inputs.

Despite its remote location, Hudson Bay is subject to anthropogenic contamination through medium to long-range atmospheric transport, as is most of Northern Canada (Barrie et al. 1992; Outridge et al. 2002; Outridge et al. 2007; Kuzyk et al. 2010a; Outridge et al. 2011). The different potential sources of anthropogenic lead contamination in the Arctic were traced using lead isotopes, as each source is characterized by a specific isotopic signature linked essentially to

124 the mined ore deposits (Sturges and Barrie 1987; Sturges et al. 1993). The sources thus identified
125 were located in Canada, the USA, Europe and Russia (Sturges and Barrie 1987; Sturges and
126 Barrie 1989).
127
128 *2.2. Sediment cores*
129 The two sediment cores used for this study (Table 1) were chosen to capture the
130 characteristics of water masses that enter Hudson Bay (station HB-6), and those that are at the
131 end of the cyclonic gyre (station A). The two cores were collected using a box-corer during the
132 MERICA cruise (étude des MERs Intérieures du Canada) in summers 2003 (station A) and 2004
133 (station HB-6). The sediment cores were collected and provided to us by Michel Starr (Maurice
134 Lamontagne Institute, Fisheries and Oceans Canada). Cores were stored in a cold room at 4°C
135 until 2006, when sub-samples were dried, crushed and stored at room temperature in the
136 laboratory. Analyses reported in this paper were performed in 2007 and 2010. Due to the
137 respective geographic locations of the two coring stations, the allochtonous material that reached
138 stations HB-6 and A originated from the western and eastern coasts of the Bay, respectively. The
139 proportion of marine organic carbon in the surface sediment in the vicinity of cores A and HB-6
140 was 80 to 85% of the total organic carbon, respectively (Kuzyk et al. 2009), stressing the
141 importance of autochthonous organic matter in the total organic sediment load of the two areas.
142

Station	Lat. (°N)	Long. (°W)	Depth (m)	Core length (cm)
HB-6	60.94°	91.78°	120	24
A	60.17°	79.00°	130	30

143 Table 1: Characteristics of the two coring stations and cores.
144
145 *2.3. Chronostratigraphy*
146 The activity of ^{210}Pb of dried and ground sediment samples was obtained indirectly by
147 measuring the decay rate of its daughter isotope ^{210}Po ($t_{1/2}$ = 138.4 days; α = 5.30 MeV) by alpha
148 spectrometry. Measurements were carried out more than 2 years after sampling to ensure that
149 secular equilibrium was reached. A ^{209}Po spike was added to the samples to determine the
150 extraction efficiency. Polonium was extracted and purified by chemical treatments (reacted

151 sequentially with HCl, HNO_3, HF and H_2O_2) and deposited on a silver disk (Flynn 1968). The
152 ^{209}Po and ^{210}Po activities were measured with a silicon surface barrier α-spectrometer
153 (EGG&ORTEC type 576A).

154 Cesium-137 was measured on dried and ground sediment samples (1 cm^3) by γ-ray
155 spectrometry at 661.6 keV (γ-ray yield = 85 %) using a low-background high-purity Ge well
156 detector (Canberra). Standard sediment (IAEA-300) was used to calibrate the yield of the
157 detector. Uncertainties were estimated for counting errors following the protocol of Not et al.
158 (2008).

159 Sedimentation accumulation rates (SAR) were calculated using the radioactive decay
160 constant (λ = 0.03114 yr^{-1}) of ^{210}Pb and the slope of the linear regression of the logarithm of
161 excess ^{210}Pb (i.e. ^{210}Pb scavenged from the water column) following the constant flux and
162 constant sedimentation model (CFCS), previously described by Sanchez-Cabeza and Ruiz-
163 Fernández (2012). Excess ^{210}Pb was estimated from the ^{210}Pb activity (Fig 2; data in the online
164 supplement) minus the supported ^{210}Pb (i.e. the ^{210}Pb produced locally from ^{226}Ra disintegration)
165 over depth. The supported ^{210}Pb was estimated using the asymptotic value of ^{210}Pb data at the
166 bottom of the core. The linear regression for sedimentation rates was applied to the middle part of
167 the core to avoid potential modern disturbance by bioturbation in the upper part of the core. We
168 considered that the topmost part of the core corresponded to the present time, as no sediment had
169 been lost during sampling. For the bottom part of the core, where no excess ^{210}Pb was measured,
170 we assumed a constant sedimentation rate.

171

172 *2.4. Isotope geochemistry*

173 In a clean-room (class 100) environment, about 50 mg of dry sedimentary material were
174 dissolved in a Teflon bomb with a mixture of HF–HNO_3 (10:1 ratio) on a hot plate at 110°C for
175 48 h, and then evaporated to dryness with a drop of HBr to help conversion to $PbBr_2$. In order to
176 ensure high purity of the separated Pb, double-pass ion chromatography was performed on AG1-
177 X8 resin in dilute HBr medium to remove matrix elements, followed by elution of Pb phase in
178 6M HCl (similar to Manhes et al., 1978). The procedural blank value was negligible (i.e. average
179 value of 42 pg Pb for 1,250,000 pg Pb of sample). Mass spectrometry was done on an IsoProbe
180 multi-collector ICP-MS, with an Aridus desolvating membrane as the introduction system. A
181 transmission of 480 V/ppm was achieved using this set-up. All isotopes of Pb were measured on

Faraday detectors with 10^{11} Ω resistors, with amplifiers cross-calibrated in the morning during the plasma warm-up time. Mass bias of samples was obtained using the NBS-991 Tl doping technique (with a Pb/Tl = 10 to 12), and the correlation between Pb and Tl mass biases was calculated from the repeated analysis of NBS-981 (Belshaw et al. 1998). Long-term reproducibility of the internal standard was better than 0.03% on isotopic ratios normalized to ^{204}Pb. The external analytical uncertainty on the isotopic ratios normalized to ^{204}Pb is on the third digit (4th digit for the ^{206}Pb/^{207}Pb ratio). Any larger change in isotopic composition was thus considered as significant. All reagents used were distilled in sub-boiling stills, and subsequently diluted with Milli-Q water.

2.5. Lead and aluminium analysis

Lead concentrations were measured on sediment core samples, and aluminum (Al) concentrations were used to normalize Pb. Aluminum was considered to be a purely lithogenic element representative of the input of the detrital component into the sediment. Indeed, very little or no Al of anthropogenic origin is thought to reach the study region, as the Hudson Bay is extremely remote and there is no significant industrial release of Al in these water. Moreover, aluminum is commonly used to normalize various elements because its natural sources highly exceed its anthropogenic sources (Daskalakis and O'Connor 1995; Heimbürger et al. 2012; Heimbürger et al. 2014; St. Pierre et al. 2015). All reagents were certified Suprapur® and provided by Merck (Darmstadt, Germany). All samples were handled under laminar airflow in a class-100 clean room. Dry bulk sediments were ground using an agate mortar. Thirty milligrams of ground sediment were weighted using a precision balance (Sartorius MC 1, accuracy 0.01 mg), and transferred to a Teflon flask. The organic and carbonate matrices were destroyed as follows: 2 mL HCl 37% and 1 mL HNO_3 65% were added to the flask and heated at 130°C for 4 h. Next, 1 mL of HF 40% and 2 mL HNO_3 65% were added to the flask to dissolve the silicate material, which was then heated at 130°C for 4 h or until complete evaporation. The residue was ultrasonically dissolved in 1 mL HNO_3 1N, and made up to 9 mL with Milli-Q water. Trace metal concentrations were measured using an Inductively Coupled Plasma Optical Emission Spectrometer (SPECTRO ARCOS™) equipped with an autosampler (CETAC ASX-260™) and an ultrasonic nebulizer (CETAC U5000AT™). Analytical procedures were validated using international certified reference material (CRM) for sediment (NCS DC 75305 and IAEA-433),

aerosol (B3-0562). Replicates of CRM were always within the quoted confidence intervals (values corresponding to "Certified" in Table 2). Detection limits (0.05 μg L^{-1} for Al, 0.01 μg L^{-1} for Pb) were defined as three times the standard deviation of blank measurements for each metal, and relative standard deviations were always <10% (results of the validation procedure are given in Table 2). The anthropogenic enrichment of samples was estimated based on the Pb/Al ratio of each sample divided by the Pb/Al ratio of the oldest samples in each core, which represent the closest to natural background value available for our region. As Al indicates terrestrial input, this index was used as a qualitative index of the sedimentary accumulation trend of non-terrestrial Pb.

	NCS-DC 75305 (μg g^{-1})	IAEA 433 (μg g^{-1})	B3-0562 (μg g^{-1})
Aluminium			
Measured (mean)	4.03 ± 0.297	80.39 ± 3.030	108.56 ± 1.37
Certified	4.08 ± 0.16	78.30 ± 4.30	107.91 ± 0.98
Lead			
Measured (mean)	22.2 ± 0.622	26.5 ± 0.329	16.94 ± 0.334
Certified	22.0 ± 1.1	26.0 ± 0.6	17.055 ± 0.195

Table 2: Certified reference material (CRM) validation results. Measurements were averaged from 3 replicates.

3. Results

3.1. Chronostratigraphy

The chronology of all cores was based on ^{210}Pb (Fig. 2, blue curves). At station A, the surface sample was lost, and the first sample was thus at 2 cm. The ^{210}Pb values decreased almost linearly from 523 Bq g^{-1} at 2 cm to 88 Bq g^{-1} at 8 cm, after which they decreased slowly until they reached the supported value of ~50 Bq g^{-1} at 27.5 cm. At station HB-6, ^{210}Pb was about 123 Bq g^{-1} at the surface of the core, and progressively increased to 176 Bq g^{-1} at 6 cm, after which it decreased linearly to reach the supported value of ~73 Bq g^{-1} at 15 cm.

We estimated the SAR using two approaches. Firstly, the CFCS model estimate yielded sedimentation rates between 0.141 ± 0.032 cm yr^{-1} (r^2 = 0.86) and 0.114 ± 0.024 cm yr^{-1}

236 ($r^2 = 0.92$) for cores A and HB-6, respectively. Secondly, ^{137}Cs values peaked at 4.5 and 5.5 cm
237 for cores A and HB-6, respectively (Fig. 2). We calculated the SAR by dividing the depth of the
238 peak depth (4.5 and 5.5 cm) by the number of years between the time of sampling and 1963.
239 These ^{137}Cs-derived sedimentation rates were consistent with the CFCS-derived rate (0.113 and
240 0.134 cm yr^{-1} for cores A and HB-6 respectively).
241 We hypothesized that the sedimentation rate was constant over the whole period covered
242 by each core, and estimated the age of the sediment by dividing its depth in the core (cm) using
243 constant sedimentation rates of 0.094 to 0.141 and 0.115 to 0.192 cm yr^{-1} for cores HB-6 and A,
244 respectively. The estimated years corresponding to different depths in each core are indicated in
245 Fig. 2 (dashed horizontal lines, corresponding to the range of sedimentation rate estimates for
246 each core).
247 Our estimated sedimentation rates are based on the assumptions that the topmost part of
248 the cores corresponded to the present time, and we used a constant sedimentation rate for the
249 bottom part. Despite the resulting uncertainties, our estimates of 0.094 to 0.141 and 0.115 to
250 0.192 cm yr^{-1} for cores HB-6 and A, respectively are consistent with values previously estimated
251 for these marine areas of Hudson Bay, i.e. 0.05 to 0.17 cm yr^{-1} (Kuzyk et al. 2009; Hare et al.
252 2010). We also observed a $^{206}Pb/^{207}Pb$ profile shift from the natural background to anthropogenic
253 value in the 1800's, a sharper shift during the 1900's, and a strong dominance of anthropogenic
254 lead in the late 1900's (Fig. 3). However, because the resulting age estimates must be taken with
255 caution, we do not discuss here the precise timing of past events, but we examine instead the
256 general temporal trends of the lead concentrations and the isotope signature.
257

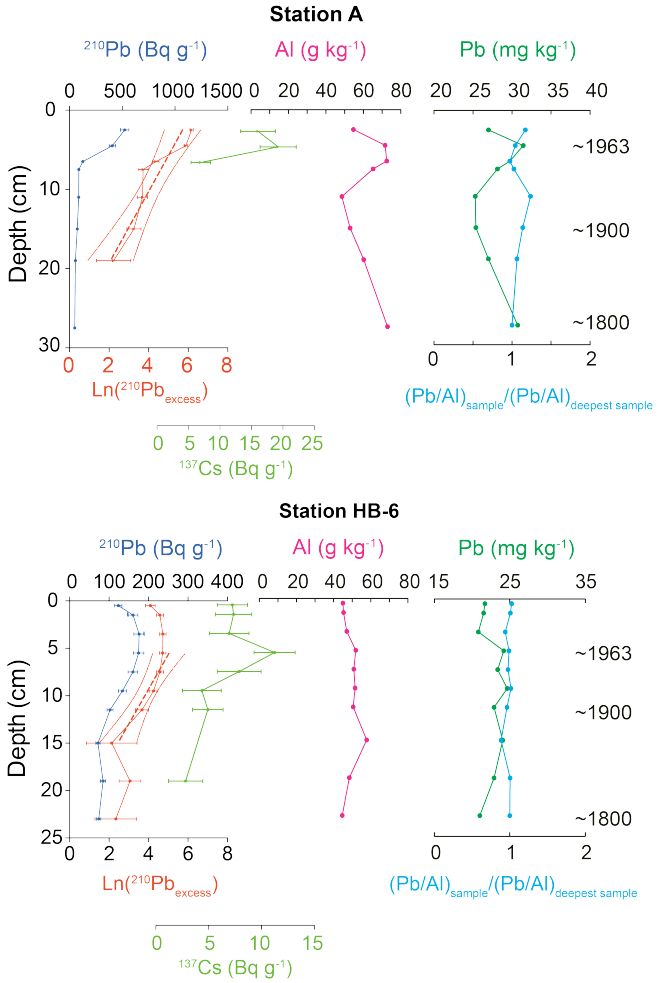

Fig. 2: Vertical profiles of ^{210}Pb, ^{137}Cs, Al and Pb in cores A (top) and HB-6 (bottom). Left panels. ^{210}Pb (Bq g^{-1}; blue, upper scale) and natural log of excess lead-210 (red, lower scale); different scales are used for the two stations. Red dashed lines: linear regressions of natural log of excess lead-210 on depth and their 95% confidence intervals. Middle panels. Profiles of Al (pink, mg kg^{-1}). Right panels. Pb concentration (green, mg kg^{-1}, upper scale), and enrichment ratio of Pb normalized to Al (blue, bottom scale). The dashed horizontal lines correspond to increasing age with depth (years are indicated), and the intervals indicate the uncertainties in our estimates. In the right panel, the enrichment ratio of Pb normalized to Al is provided on a 0-to-2 scale, where 1 indicates no enrichment compared to the oldest value recorded at the site, 2 represents a 2-time enrichment, and a value between 0 and 1 represents a decrease of Pb/Al compared to the oldest recorded value.

3.2. Lead geochemistry

Bottom-to-top variations in concentrations of Al and Pb were different in the two cores (Fig. 2, left and middle panels). At station A, Al and Pb increased by ~30% from 10 to 4 cm (i.e.

from the 1800's to the early 1900's), after which they both decreased in the topmost samples. At station HB-6, there was no strong vertical variation in either the Al or Pb profile. In both cores, variations in the enrichment ratio normalized to Al were small (Fig. 2, right panel). There was a strong positive correlation between Pb and Al in the two cores (station A: r = 0.95, Prob <0.0005; station HB-6: r = 0.83, Prob <0.005).

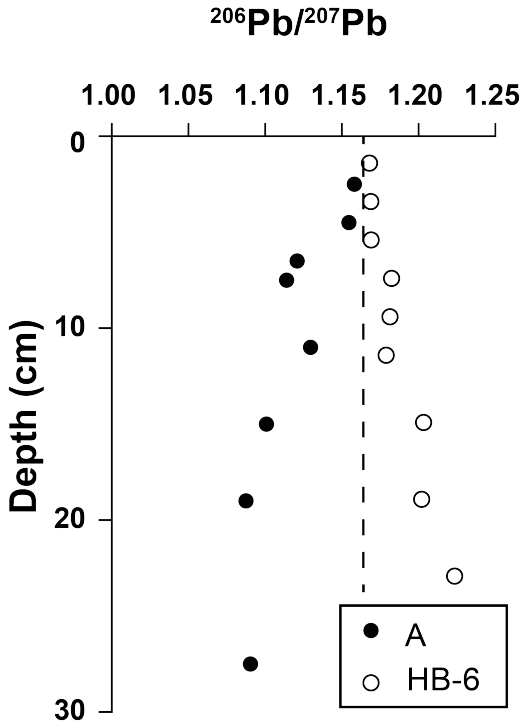

Fig. 3: $^{206}Pb/^{207}Pb$ ratio in cores HB-6 and A. The dashed vertical line represents the isotopic value of the Arctic anthropogenic Pb (1.16; Sturges et al. 1993). The error bars are smaller than the dots (see text for details).

Concerning the isotopes, there was a shift in $^{206}Pb/^{207}Pb$ in core A from 1.09 at the bottom to about 1.16 in the topmost centimeters (Fig. 3). In core HB-6, the pattern was opposite, with the bottom-to-top ratio shifting from 1.22 to 1.17. The isotopic values of the two cores converged at the top. We also investigated the variations in ^{204}Pb, ^{206}Pb and ^{208}Pb as it had been suggested that normalizing ^{206}Pb and ^{208}Pb to ^{204}Pb generally allows to distinguish between three mixed end-members (Ellam 2010). In the scatter diagram of $^{208/204}Pb$ *vs* $^{206/204}Pb$ (Fig. 4; values in the supplemental material), the ratios from the two cores are very far apart for the oldest samples and progressively converge toward similar values for the most recent samples.

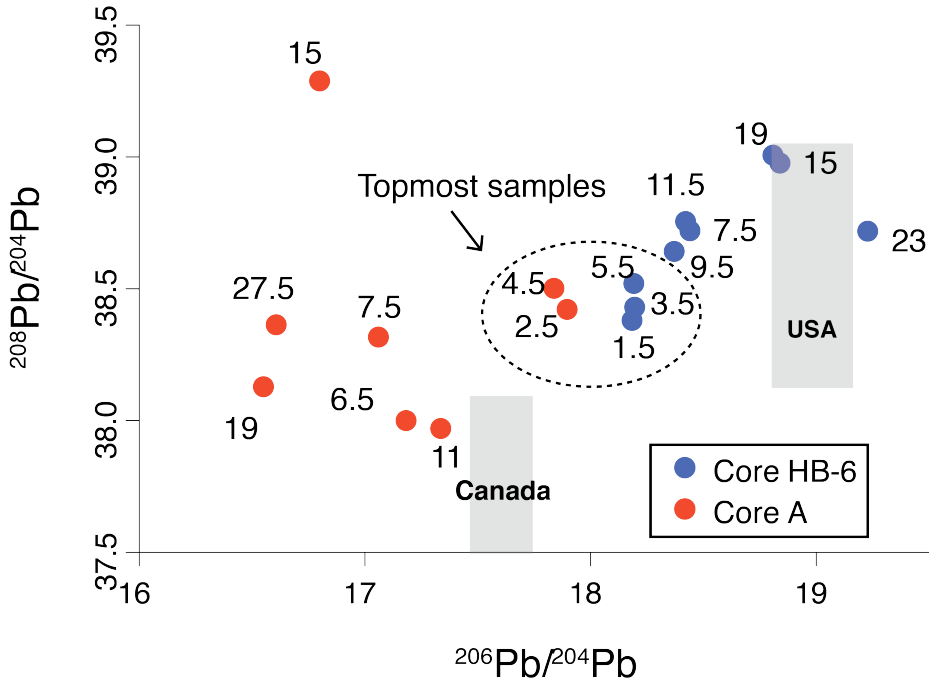

Fig. 4. Plot of the isotopic ratios $^{208/204}$Pb on $^{206/204}$Pb, along with national aerosol averaged values for two different potential source regions (grey boxes), i.e. Canada and the USA in the 1980's (Sturges and Barrie 1987; Graney et al. 1995; Poirier 2006). Each sample is labelled with its depth (in cm) in its core to highlight the temporal convergence of the isotope ratios from the two cores toward the same values.

4. Discussion

4.1. Historical variations in the sources of Pb

The Hudson Bay is characterized by intense sediment resuspension due to postglacial isostatic rebound (Hare et al. 2008; Kuzyk et al. 2009), which can dilute anthropogenic inputs in surface sediments (Hare et al. 2010). This could partly mask the sedimentary record of anthropogenic Pb, and thus prevent the use of our sediment records to investigate the vertical export of Pb during the last centuries. However, our cores clearly recorded Pb of anthropogenic origin, as shown by the convergent trend toward the anthropogenic value of 1.16 (Sturges and Barrie 1987) in Figure 3, and are thus suitable for investigating the vertical export dynamics of anthropogenic Pb as shown by the ^{210}Pb chronology, which was corroborated by a secondary stratigraphic marker (^{137}Cs).

Because Al in sediments traces the terrestrial inputs, the correlation between Pb and Al provides information on the importance of lithogenic inputs in the accumulation of Pb (Brumsack

2006). The strong positive correlations of Pb and Al in the two cores (Section 3.2) indicate that the historical Pb accumulation was strongly controlled by terrestrial inputs. In addition, the vertical export of terrestrial or atmospheric Pb from surface waters to the sediment would have different effects on Pb concentration normalized to Al, i.e. terrestrial Pb would be deposited together with terrestrial Al, hence constant Pb normalized to Al, whereas atmospheric Pb would not be deposited together with terrestrial Al, hence higher Pb normalized to Al (Daskalakis and O'Connor 1995; Heimbürger et al. 2012; Heimbürger et al. 2014). Moreover, enrichment factors of mercury relative to aluminium have been similarly used to identify the source of mercury (atmosphere against underlying soils) by St. Pierre et al. (2015). At our two stations, there were no strong variations in the enrichment ratio of Pb normalized to Al along the cores, indicating that the sedimentary accumulation of airborne Pb remained constant during the last 200 years in the two cores.

Irrespective of the isotope considered, the two cores were characterized by a trend (i.e. older to recent) that converged toward a value half way between typical historical Canadian and USA lead emissions (Figs. 3 and 4). The oldest samples in the two cores were characterized by opposite $^{206}Pb/^{207}Pb$, $^{206}Pb/^{204}Pb$ and $^{208}Pb/^{204}Pb$ isotopic signatures (Figs. 3 and 4), meaning that early-industrial Pb inputs (i.e. between 1800 and 1900) originated from different sources in the western and eastern parts of Hudson Bay. The temporal trends of $^{206}Pb/^{204}Pb$ and $^{208}Pb/^{204}Pb$ in core HB-6 are similar to those observed in two Hudson Bay lakes (Outridge et al. 2002), suggesting similar early-industrial sources of lead on the western side of the Bay. The early-industrial $^{206}Pb/^{207}Pb$ isotopic signature was different in cores A and HB-6 (1.10 and 1.22, respectively), on the eastern and western sides of the Bay, respectively. This probably reflected the spatial heterogeneity that exists in the different potential sources of Pb (with different isotopic signatures) in the Canadian shield, which surrounds most of Hudson Bay (GEOROC 2003). The isotopic ratio values toward which the two cores converged were the same as in surrounding lakes on the two sides of Hudson Bay (Fig. 3 in this study, and Figs. 6 and 7 in Outridge et al. 2002). Irrespective of the early-industrial sources, the fact that the isotopic composition in the two cores started with different values and converged toward a single value indicates that both cores recorded the imprint of medium to long-range anthropogenic Pb deposition during the last century.

343 *4.2. Effect of primary productivity on the sedimentary Pb record*

344 Local anthropogenic inputs of metals are low in the Hudson Bay area because of its
345 remote location and the scarcity of industries. Hence, medium to long-range atmospheric
346 transport was presumably the main source of anthropogenic contaminants. A small increase from
347 25 to 30 mg kg^{-1} in Pb concentration was observed in sediment core A around 6 and 7 cm (Fig. 2).
348 However, because a similar increase was also observed in Al, Pb normalized to Al was mostly
349 constant, which suggested that Pb was of terrestrial origin. This is consistent with the slight
350 reduction in $^{206}Pb/^{207}Pb$ near 6 and 7 cm in core A indicating a transient return to more terrestrial
351 (background) values. This transient increase in terrestrial input could be related to increased
352 precipitation due to the climatic variability of Hudson Bay (Guiot 1987). In core HB-6, the record
353 showed no sign of increase in either Pb concentration or Pb/Al, suggesting relatively constant Pb
354 input (terrestrial and atmospheric) during the last two centuries in this part of the bay. The ~20%
355 increase in Pb concentration in core A is much smaller than the three- to five-fold increase in Pb
356 concentration in the recent sediments (last century) of two lakes in the Hudson Bay (Outridge et
357 al. 2002). The observed increase in Pb in lake sediments was attributed by Outridge et al. (2002)
358 to medium to long-range atmospheric inputs of anthropogenic Pb originating from Eurasia and
359 North America. Because waters of the lakes and Hudson Bay should have been both exposed to
360 similar inputs of atmospheric materials, the difference in Pb accumulation between the two
361 environments indicates that the transfer mechanisms of Pb to the sediment where different in the
362 two environments, assuming no diagenetic or post-sampling effect on Pb concentrations. The
363 $^{206}Pb/^{207}Pb$ isotopic values (Fig. 3) show, for the cores on the two sides of the Hudson Bay, an
364 apparent progressive overprint of anthropogenic lead (from bottom to top of cores) during the
365 1900's, whose isotopic ratio reflects a mixed Canada-USA aerosol origin ($^{206}Pb/^{207}Pb$ = 1.16-
366 1.17; Sturges and Barrie 1987). In other words, despite a globally increased atmospheric import
367 of anthropogenic lead (Nriagu 1996), the amount of Pb deposited in Hudson Bay's sediment did
368 not change dramatically during the last century, but the sources of emission changed as shown by
369 changes in the isotope ratios. This indicates that sedimentary accumulation of anthropogenic Pb
370 was limited in Hudson Bay by a factor that acted differently in the bay than in surrounding lakes.

371 Assuming a typical sinking velocity of 20 to 200 m d^{-1} for Pb when packaged within
372 biogenic aggregates (Alldredge and Gotschalk 1988; Armstrong et al. 2009; McDonnell and
373 Buesseler 2010), i.e. when sedimentation is driven by biological productivity, surface Pb would

374 reach 250 m (i.e. the maximum depth of Hudson Bay) within less than 15 days (the depths of
375 coring sites HB-6 and A were 120 and 130 m, respectively). Hence even if the estimates of the
376 residence time of Hudson surface waters vary over a wide range in the literature (i.e. from one
377 month to 6 years, Section 2.1), Pb packaged within biogenic aggregates should sediment within
378 the Bay. As a result, the only ways by which Pb would have not reached the sediment should
379 have been either a lack of aggregation due to very low biological productivity, and/or a very low
380 sinking velocity of the Pb-containing aggregates, i.e. $<<20$ m d^{-1}. These two conditions would
381 have led Pb to be flushed out of the bay.
382 Our results and previously published data show that the sedimentary accumulation of Pb
383 in the last century was not the same in the records of low-productivity Hudson Bay as in the high-
384 productivity nearby lakes, whereas the recent isotopic composition was the same in sediments
385 from both Hudson Bay and the surrounding lakes (Outridge et al. 2002). Hence, we cannot reject
386 our initial hypothesis that primary productivity was the main forcing factor determining the
387 sedimentation of airborne matter. This hypothesis is consistent with the suggestion from previous
388 studies that sedimentary sequences in Hudson Bay did not always record directly the atmospheric
389 deposition of allochthonous matter, but could be affected by low primary productivity. For
390 example and similarly to our Pb observations, it was recently suggested that the sedimentation of
391 polychlorinated biphenyl (PCBs) was exceptionally low in Hudson Bay, because the very low
392 productivity in the Bay and the resulting weak downward flux of organic matter inhibited the
393 transfer of PCBs from surface to depth and, therefore, their sedimentation (Kuzyk et al. 2010a).
394 Such a relationship between primary productivity and the downward flux of aggregates may be a
395 typical feature of many environments in the world ocean (Passow 2004; Heimbürger et al. 2014).
396 The conceptual model in Fig. 5 summarizes the above ideas, illustrating the early-
397 industrial and post-industrial situations in Hudson Bay. In the early-industrial model, atmospheric
398 inputs of Pb were low, and this Pb was characterized by the local isotopic signature α. Most Pb,
399 perhaps all, was exported downwards and accumulated in the sediment after being scavenged by
400 organic particles, thus transferring the isotopic signature of Pb from surface waters to the
401 sediment. The post-industrialization model is characterized by a higher rate of Pb input from the
402 atmosphere to the surface water due to the enhanced medium to long-range transport of
403 anthropogenic Pb (Outridge et al. 2002). This Pb is characterized by the different isotopic
404 signature β, which reflects its mixed local and anthropogenic origins. The similar concentration

of Pb accumulated in the sediment is explained by a limitation of its export by the low primary productivity of Hudson Bay, which restricts the availability of organic particles to scavenge Pb and export it to the sediment. As a consequence, despite a likely increase in atmospheric deposition of Pb with increased industrialization, its accumulation was similar after and before industrialization, but its isotopic signature was different in the two periods.

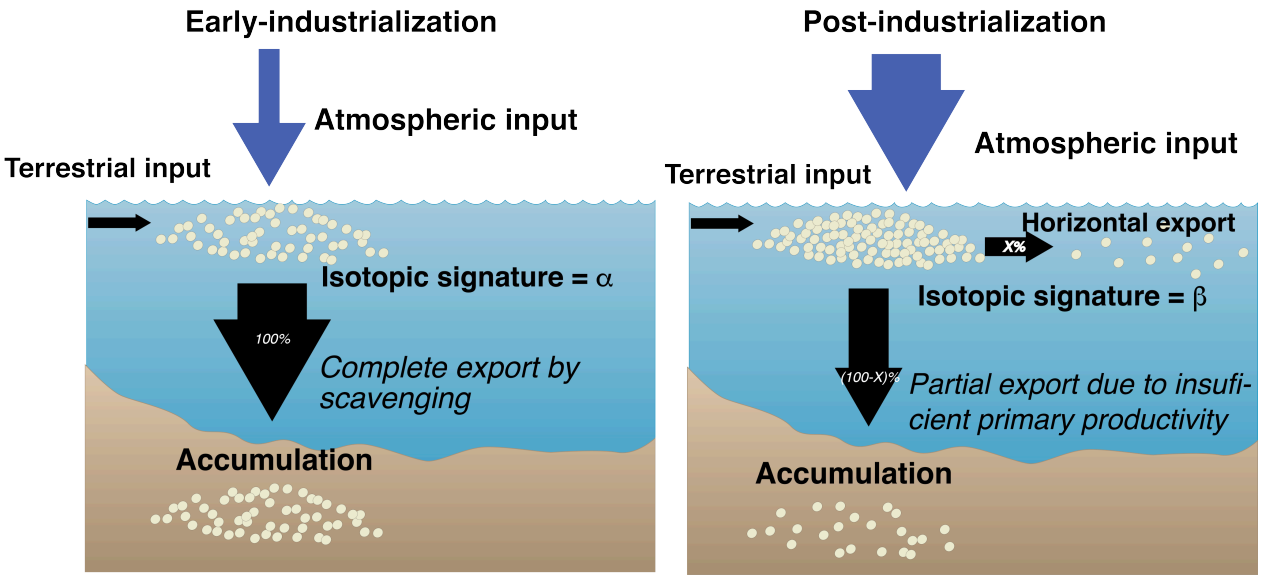

Fig. 5. Schematic representation of our hypothesis on the atmospheric and water-column fluxes of contaminants before and after industrialization in Hudson Bay. The illustrated mechanisms explain both the absence of difference in Pb sedimentary accumulation, and the change in the isotopic signatures of sediments from the early-industrial to the post-industrial period.

Enhanced atmospheric inputs of contaminants in the last century were not significantly recorded in Hudson Bay sediments, presumably because of the exceptionally low productivity of the Bay (Kuzyk et al. 2009), which prevented the efficient transfer of chemical elements from the water column to the sediment. However, the signature of the Pb isotopes suggests a shift from local input to medium to long-range anthropogenic inputs during the 20th century, which thus recorded the signature of the last century. This is consistent with our hypothesis that low primary productivity was the main forcing factor that determined the sedimentation of atmospherically-deposited matter in Hudson Bay during the last century. This observation is globally significant as Hudson Bay is extremely sensitive to warming, with an increase of 0.47°C per decade over the last 50 years (Mulder et al. 2016). Warming will lead to increased river discharge, which could

enhance primary productivity in the Hudson Bay because river discharge promotes the upwelling of deep waters (Kuzyk et al. 2010a; Kuzyk et al. 2010b). If Arctic regions are currently warming up, one may expect increasing fluxes of nutrients to Hudson Bay, in the northern part of Canada. It may therefore also be expected that the magnitude of primary productivity in Hudson Bay will increase as well, which would lead to an increase in export fluxes of atmospherically-deposited contaminants, once packaged with particulate biogenic matter.

4.3. Possible effect of transparent exopolymer particles (TEP)

It was mentioned above that one of the possible explanations to our observations was that the Pb-containing aggregates sank at very low velocity. This could have occurred if the aggregates formed in Hudson Bay had been neutrally buoyant, and had thus remained in surface waters long enough to be flushed out of the Bay. While there are multiple factors that can influence the particle settling velocity (Maggi 2013), the accumulation of positively buoyant transparent exopolymer particles (TEP) in oligotrophic surface waters is hypothesized to contribute to slowing down the downward export flux (Azetsu-Scott and Passow 2004, Mari et al. 2017).

The increase of TEP volume concentration in surface waters is a significant feature in some oligotrophic waters, e.g. the Mediterranean Sea (Mari et al. 2001; Bar-Zeev et al. 2011), the Pacific Ocean (Wurl et al. 2011; Kodama et al. 2014), and Hudson Bay (Michel et al. 2006). The limited TEP dataset for Hudson Bay is characterized by a sub-surface maximum around 50 m where it co-occurs with the chlorophyll *a* maximum, suggesting a link between the two (Michel et al. 2006). Nutrient limitation increases the production of TEP by phytoplankton and lowers their bacterial degradation, and the two processes contribute to TEP accumulation in surface waters (Mari et al. 2001, 2017). Owing to their high stickiness, TEP are often seen as a catalyst of aggregation, and thus a key component for the formation of fast-sinking aggregates (Passow et al. 2001), but (Mari et al. 2017) proposed that a system with high volume concentration of low-density TEP and low concentration of dense particles in surface waters should be characterized by low downward POC export (Mari et al. 2017). The latter conditions are those observed during periods of severe oligotrophy in Hudson Bay, where the accumulation of TEP in surface waters could have enhanced the residence time of TEP-associated elements (e.g. Pb) and particles

(e.g. mineral dust) in surface, thus favoring their horizontal export out of the bay instead of downward export.

Acknowledgements

All data used in this paper are available in the online supplement. Funding was provided by the Fonds Québécois de la Recherche sur la Nature et les Technologies through an international doctoral internship grant awarded to BT. We thank M. Starr, and the monitoring program for Canadian interior seas (MERICA) funded by the Canadian Department of Fisheries and Oceans, Natural Resources Canada, and the Canadian Coast Guard for providing the cores and the ship time. We are grateful to R. Losno (Institut de physique du globe de Paris) for his assistance with trace metal analyses. We are thankful to the two anonymous reviewers for their constructive input.

References

ACIA (2004) Impacts of a Warming Arctic: Arctic Climate Impact Assessment. ACIA Overv. Rep. 140.

Alldredge AL, Gotschalk C (1988) In situ settling behavior of marine snow. Limnol Oceanogr 33:339–35. doi: 10.4319/lo.1988.33.3.0339

Alldredge AL, Silver MW (1988) Characteristics, dynamics and significance of marine snow. Prog Oceanogr 20:41–82. doi: 10.1016/0079-6611(88)90053-5

Armstrong RA, Lee C, Hedges JI, et al (2002) A new, mechanistic model for organic carbon fluxes in the ocean based on the quantitative association of POC with ballast minerals. 49:219–236. doi: 10.1016/S0967-0645(01)00101-1

Armstrong RA, Peterson ML, Lee C, Wakeham SG (2009) Settling velocity spectra and the ballast ratio hypothesis. Deep Res Part II Top Stud Oceanogr 56:1470–1478. doi: 10.1016/j.dsr2.2008.11.032

Azetsu-Scott K, Passow U (2004) Ascending marine particles: Significance of transparent exopolymer particles (TEP) in the upper ocean. Limnol Oceanogr 49:741–748. doi: 10.4319/lo.2004.49.3.0741

Bar-Zeev E, Berman T, Rahav E, et al (2011) Transparent exopolymer particle (TEP) dynamics in the eastern Mediterranean Sea. Mar Ecol Prog Ser 431:107–118. doi: 10.3354/meps09110

Barrie LA, Gregor D, Hargrave B, et al (1992) Arctic contaminants: sources, occurrence and pathways. Sci Total Environ 122:1–74. doi: 10.1016/0048-9697(92)90245-N

Barrie LA, Hoff RM, Daggupaty SM (1981) The influence of mid-latitudinal pollution sources on haze in the Canadian arctic. Atmos Environ 15:1407–1419. doi: 10.1016/0004-6981(81)90347-4

Belshaw N, Freedman P, O'Nions R, et al (1998) A new variable dispersion double-focusing plasma mass spectrometer with performance illustrated for Pb isotopes. Int J Mass Spectrom 181:51–58. doi: 10.1016/S1387-3806(98)14150-7

Boyce DG, Lewis MR, Worm B (2010) Global phytoplankton decline over the past century. Nature 466:591–596. doi: 10.1038/nature09268

Brumsack HJ (2006) The trace metal content of recent organic carbon-rich sediments: Implications for Cretaceous black shale formation. Palaeogeogr Palaeoclimatol Palaeoecol 232:344–361. doi: 10.1016/j.palaeo.2005.05.011

Buat-Ménard P, Davies J, Remoudaki E, et al (1989) Non-steady-state biological removal of atmospheric particles from Mediterranean surface waters. Nature 340:131–134. doi: 10.1038/340131a0

Burd AB, Jackson GA (2009) Particle aggregation. Ann Rev Mar Sci 1:65–90. doi: 10.1146/annurev.marine.010908.163904

Daskalakis KD, O'Connor TP (1995) Normalization and elemental sediment contamination in the coastal United States. Environ Sci Technol 29:470–477. doi: 10.1021/es00002a024

De Angelis M, Gaudichet A (1991) Saharan dust deposition over Mont Blanc (French Alps) during the last 30 years. Tellus 43B:61–75. doi: 10.1034/j.1600-0889.1991.00005.x

Deuser WG, Brewer PG, Jickells TD, Commeau RF (1983) Biological control of the removal of abiogenic particles from the surface ocean. Science (80-) 219:388–391. doi: 10.1126/science.219.4583.388

Ellam RM (2010) The graphical presentation of lead isotope data for environmental source apportionment. Sci Total Environ 408:3490–3492. doi: 10.1016/j.scitotenv.2010.03.037

Flynn WW (1968) The determination of low levels of polonium-210 in environmental materials. Anal Chim Acta 43:221–227. doi: 10.1016/S0003-2670(00)89210-7

Fowler SW, Buat-Ménard P, Yokoyama Y, et al (1987) Rapid removal of Chernobyl fallout from Mediterranean surface waters by biological activity. Nature 329:56–58. doi: 10.1038/329056a0

Francois R, Honjo S, Krishfield R, Manganini S (2002) Factors controlling the flux of organic carbon to the bathypelagic zone of the ocean. Global Biogeochem Cycles 16:1087. doi: 10.1029/2001gb001722

Gačić M, Civitarese G, Miserocchi S, et al (2002) The open-ocean convection in the Southern Adriatic: A controlling mechanism of the spring phytoplankton bloom. Cont Shelf Res 22:1897–1908. doi: 10.1016/S0278-4343(02)00050-X

GEOROC (2003) Geochemistry of Rocks of the Oceans and Continents. In: MPI für Chemie/Max-Planck Inst. für Chemie, Mainz, Ger.

Graney JR, Halliday AN, Keeler GJ, et al (1995) Isotopic record of lead pollution in lake sediments from the northeastern United States. Geochim Cosmochim Acta 59:1715–1728. doi: 10.1016/0016-7037(95)00077-D

Granskog MA, Macdonald RW, Kuzyk ZZA, et al (2009) Coastal conduit in southwestern Hudson Bay (Canada) in summer: Rapid transit of freshwater and significant loss of colored dissolved organic matter. J Geophys Res Ocean 114:C08012. doi: 10.1029/2009JC005270.

Guiot J (1987) Reconstruction of seasonal temperatures in Central Canada since A.D. 1700 and detection of the 18.6- and 22-year signals. Clim Change 10:249–268. doi: 10.1007/BF00143905
Hare AA, Stern GA, Kuzyk ZZA, et al (2010) Natural and anthropogenic mercury distribution in marine sediments from Hudson Bay, Canada. Environ Sci Technol 44:5805–5811. doi: 10.1021/es100724y
Hare A, Stern GA, Macdonald RW, et al (2008) Contemporary and preindustrial mass budgets of mercury in the Hudson Bay Marine System: The role of sediment recycling. Sci Total Environ 406:190–204. doi: 10.1016/j.scitotenv.2008.07.033
Heimbürger L-E, Cossa D, Thibodeau B, et al (2012) Natural and anthropogenic trace metals in sediments of the Ligurian Sea (Northwestern Mediterranean). Chem Geol 291:141–151. doi: 10.1016/j.chemgeo.2011.10.011
Heimbürger LE, Lavigne H, Migon C, et al (2013) Temporal variability of vertical export flux at the DYFAMED time-series station (Northwestern Mediterranean Sea). Prog Oceanogr 119:59–67. doi: 10.1016/j.pocean.2013.08.005
Heimbürger LE, Migon C, Losno R, et al (2014) Vertical export flux of metals in the Mediterranean Sea. Deep Res Part I Oceanogr Res Pap 87:14–23. doi: 10.1016/j.dsr.2014.02.001
Jackson GA, Burd AB (1998) Aggregation in the marine environment. Environ Sci Technol 32:2805–2814. doi: 10.1021/es980251w
Jones EP, Anderson LG (1994) Northern Hudson Bay and Foxe Basin: Water masses, circulation and productivity. Atmosphere-Ocean 32:361–374. doi: 10.1080/07055900.1994.9649502
Kodama T, Kurogi H, Okazaki M, et al (2014) Vertical distribution of transparent exopolymer particle (TEP) concentration in the oligotrophic western tropical North Pacific. Mar Ecol Prog Ser 513:29–37. doi: 10.3354/meps10954
Kuzyk ZZA, Macdonald RW, Johannessen SC, et al (2009) Towards a sediment and organic carbon budget for Hudson Bay. Mar Geol 264:190–208. doi: 10.1016/j.margeo.2009.05.006
Kuzyk ZZA, MacDonald RW, Johannessen SC, Stern GA (2010a) Biogeochemical controls on PCB deposition in Hudson Bay. Environ Sci Technol 44:3280–3285. doi: 10.1021/es903832t
Kuzyk ZZA, Macdonald RW, Tremblay JÉ, Stern GA (2010b) Elemental and stable isotopic constraints on river influence and patterns of nitrogen cycling and biological productivity in Hudson Bay. Cont Shelf Res 30:163–176. doi: 10.1016/j.csr.2009.10.014
Lampitt RS, Salter I, de Cuevas BA, et al (2010) Long-term variability of downward particle flux in the deep northeast Atlantic: Causes and trends. Deep Res Part II Top Stud Oceanogr 57:1346–1361. doi: 10.1016/j.dsr2.2010.01.011
Macdonald RW, Harner T, Fyfe J (2005) Recent climate change in the Arctic and its impact on contaminant pathways and interpretation of temporal trend data. Sci. Total Environ. 342:5–86.
Maggi F (2013) The settling velocity of mineral, biomineral, and biological particles and aggregates in water. J Geophys Res Ocean 118:2118–2132. doi: 10.1002/jgrc.20086
Manhes G, Minster JF, Allègre CJ (1978) Comparative uranium-thorium-lead and rubidium-strontium study of the Saint Sèverin amphoterite: consequences for early solar system chronology. Earth Planet Sci Lett 39:14–24. doi: 10.1016/0012-821X(78)90137-1
Mari X, Beauvais S, Lemée R, Pedrotti ML (2001) Non-Redfield C:N ratio of transparent exopolymeric particles in the northwestern Mediterranean Sea. Limnol Oceanogr 46:1831–1836. doi: 10.4319/lo.2001.46.7.1831
Mari X, Passow U, Migon C, et al (2017) Transparent exopolymer particles: Effects on carbon cycling in the ocean. Prog Oceanogr 151:13–37. doi: http://dx.doi.org/10.1016/j.pocean.2016.11.002
McDonnell AMP, Buesseler KO (2010) Variability in the average sinking velocity of marine particles. Limnol Oceanogr 55:2085–2096. doi: 10.4319/lo.2010.55.5.2085
Michel C, Hamilton J, Hansen E, et al (2015) Arctic Ocean outflow shelves in the changing Arctic: A review and perspectives. Prog Oceanogr 139:66–88. doi: 10.1016/j.pocean.2015.08.007
Michel C, Lapoussiere A, LeBlanc B, Starr M (2006) Transparent expopolymeric substances (TEP) in Hudson Bay during fall: significance and potential roles. http://www.arcticnet.ulaval.ca/pdf/posters_2006/michel_eT_al.pdf. Accessed 22 Aug 2016
Migon C, Sandroni V, Marty JC, et al (2002) Transfer of atmospheric matter through the euphotic layer in the northwestern Mediterranean: Seasonal pattern and driving forces. Deep Res Part II Top Stud Oceanogr 49:2125–2141. doi: 10.1016/S0967-0645(02)00031-0
Miller GH, Lehman SJ, Refsnider KA, et al (2013) Unprecedented recent summer warmth in Arctic Canada. Geophys Res Lett 40:5745–5751. doi: 10.1002/2013GL057188
Mulder CPH, Iles DT, Rockwell RF (2016) Increased variance in temperature and lag effects alter phenological responses to rapid warming in a subarctic plant community. Glob. Chang. Biol.

Not C, Hillaire-Marcel C, Ghaleb B, et al (2008) 210 Pb– 226 Ra– 230 Th systematics in very low sedimentation rate sediments from the Mendeleev Ridge (Arctic Ocean). Can J Earth Sci 45:1207–1219. doi: 10.1139/E08-047

Nriagu JO (1996) A History of Global Metal Pollution. Science (80-) 272:223–0. doi: 10.1126/science.272.5259.223

Outridge P., Hermanson M., Lockhart W. (2002) Regional variations in atmospheric deposition and sources of anthropogenic lead in lake sediments across the Canadian Arctic. Geochim Cosmochim Acta 66:3521–3531. doi: 10.1016/S0016-7037(02)00955-9

Outridge PM, Rausch N, Percival JB, et al (2011) Comparison of mercury and zinc profiles in peat and lake sediment archives with historical changes in emissions from the Flin Flon metal smelter, Manitoba, Canada. Sci Total Environ 409:548–563. doi: 10.1016/j.scitotenv.2010.10.041

Outridge PM, Sanei LH, Stern G a, et al (2007) Evidence for control of mercury accumulation rates in Canadian High Arctic lake sediments by variations of aquatic primary productivity. Environ Sci Technol 41:5259–65.

Passow U (2004) Switching perspectives: Do mineral fluxes determine particulate organic carbon fluxes or vice versa? Geochemistry Geophys Geosystems 5:1–5. doi: 10.1029/2003GC000670

Passow U, Carlson CA (2012) The biological pump in a high CO2 world. Mar Ecol Prog Ser 470:249–271. doi: 10.3354/meps09985

Passow U, Shipe RF, Murray A, et al (2001) The origin of transparent exopolymer particles (TEP) and their role in the sedimentation of particulate matter. Cont Shelf Res 21:327–346. doi: 10.1016/S0278-4343(00)00101-1

Poirier A (2006) Re-Os and Pb isotope systematics in reduced fjord sediments from Saanich Inlet (Western Canada). Earth Planet Sci Lett 249:119–131. doi: 10.1016/j.epsl.2006.06.048

Prinsenberg SJ (1984) Freshwater contents and heat budgets of James Bay and Hudson Bay. Cont Shelf Res 3:191–200. doi: 10.1016/0278-4343(84)90007-4

Prinsenberg SJ (1986) Chapter 10 The Circulation Pattern and Current Structure of Hudson Bay. In: Martini I (ed) Canadian Inland seas: Elsevier Oceanography Series. Elsevier B.V., Amsterdam, The Netherlands, pp 187–204

Rahn KA, Borys RD, Shaw GE (1977) The Asian source of Arctic haze bands. Nature 268:713–715. doi: 10.1038/268713a0

Sanchez-Cabeza JA, Ruiz-Fernández AC (2012) 210Pb sediment radiochronology: An integrated formulation and classification of dating models. Geochim Cosmochim Acta 82:183–200. doi: 10.1016/j.gca.2010.12.024

Saucier FJ, Dionne J (1998) A 3-D coupled ice-ocean model applied to Hudson Bay, Canada: The seasonal cycle and time-dependent climate response to atmospheric forcing and runoff. J Geophys Res Ocean 103:27689–27705. doi: 10.1029/98JC02066

St. Pierre KA, St. Louis VL, Kirk JL, et al (2015) Importance of Open Marine Waters to the Enrichment of Total Mercury and Monomethylmercury in Lichens in the Canadian High Arctic. Environ Sci Technol 49:5930–5938. doi: 10.1021/acs.est.5b00347

Sturges WT, Barrie LA (1989) Stable lead isotope ratios in arctic aerosols: evidence for the origin of arctic air pollution. Atmos Environ 23:2513–2519. doi: 10.1016/0004-6981(89)90263-1

Sturges WT, Barrie LA (1987) Lead 206/207 isotope ratios in the atmosphere of North America as tracers of US and Canadian emissions. Nature 329:144–146.

Sturges WT, Hopper JF, Barrie LA, Schnell RC (1993) Arctic air, snow and ice chemistryStable lead isotope ratios in Alaskan arctic aerosols. Atmos Environ Part A Gen Top 27:2865–2871. doi: http://dx.doi.org/10.1016/0960-1686(93)90317-R

Turner JT (2002) Zooplankton fecal pellets, marine snow and sinking phytoplankton blooms. Aquat Microb Ecol 27:57–102. doi: 10.3354/ame027057

Turner JT (2015) Zooplankton fecal pellets, marine snow, phytodetritus and the ocean's biological pump. Prog Oceanogr 130:205–248. doi: 10.1016/j.pocean.2014.08.005

Wurl O, Miller L, Vagle S (2011) Production and fate of transparent exopolymer particles in the ocean. J Geophys Res Ocean 116:C00H13. doi: 10.1029/2011JC007342

Yool A, Popova EE, Coward AC, et al (2013) Climate change and ocean acidification impacts on lower trophic levels and the export of organic carbon to the deep ocean. Biogeosciences 10:5831–5854. doi: 10.5194/bg-10-5831-2013